Lignocellulosic residues as catalysts for CO_2 fixation: complementary experimental and computational approaches

Mohamed Said El Ouahabi,[a,b] Md Bin Yeamin[a,1], Raquel Rivas,[a] Farid El Guemmout,[b] Mar Reguero,[a,*] Anna M. Masdeu-Bultó[a,*] and Ali Aghmiz.[b,*]

[a] *Department Physical and Inorganic Chemistry. University Rovira i Virgili. Marcel·lí Domingo, s/n. 43007 Tarragona (Spain).*

[b] *Département de Chimie, Faculté des Sciences, University Abdelmalek Essaadi, M'hannech II, B.P. 2121. 93030 Tétouan (Morocco).*

+34 977558779

+34 977558763

annamaria.masdeu@urv.cat

http://www.urv.cat/dqfi/en_index.html

Lignocellulosic wastes obtained from vegetal residues in combination with nucleophiles were used as catalysts for carbon dioxide fixation in epoxides to form cyclic carbonates. An adequate combination of residues and nucleophiles was essential to obtain the carbonates at very low catalyst/nucleophile ratio under mild conditions. The best binary systems were formed by olive bones, grape waste, date pit and corn leaves husk residues with tetrabutylammonium bromide (TBAB). High conversions in the cycloaddition of CO_2 to propylene oxide (76-84%) and 1,2-epoxyhexane (68-79%) were achieved at very low nucleophile loading (0.47 mol% respect the substrate) under mild conditions (95 ºC and 10 atm of CO_2). The vegetal wastes were stable under catalytic conditions and could be recycled after adequate supporting the nucleophile TBAB in silica gel. The mechanistic computational study carried out with Density Functional Theory (DFT) calculations on model catalysts describes the contribution of individual lignin and cellulosic components to the experimental substrate conversion into cyclic carbonate. The energy barriers obtained and the experimental data suggest that the contribution of lignin to the total catalytic activity (barrier energy of 9.94 kcal/mol) may be more important than the contribution of cellulose (energy barrier 11.89 kcal/mol).

carbon dioxide, carbonates, lignocellulosic materials, epoxides, DFT calculations

[1] *Permanent Address: IUBAT University, Sector-10, Uttara, Dhaka 1230, Uttara Model Town, Dhaka, Bangladesh.*

Introduction

The use of organocatalysts based on natural products to synthesize chemicals is considered as cutting-edge technology due to the safe, non-toxic, and sustainable nature of these products as compared to other catalysts. Lignocellulosic materials obtained from biomass are a sustainable source of resources by chemical transformation (Corma et al. 2007). Moreover, the high functionalized surface of cellulose and lignin-based products is very appropriate to prepare materials for multiple applications (Thomas et al. 2018). Thus, there are many examples in the literature of the use of cellulose derivatives as, for example, bio-based hybrid materials for photocatalysts (Colmenares and Kuna 2017), bio-polymer support for metal catalysts (Dong et al. 2019) or as catalysts for carbon dioxide fixation (Liu et al. 2019). This later application is especially interesting since carbon dioxide is one of the greenhouse gases, which emissions and accumulation cause significant and negative effects on the global environment (Ripple et al. 2017). The use of CO_2, taking advantage of its abundance, availability, non-toxicity and recyclability, represents an option that might contribute to reducing CO_2 accumulation in the atmosphere (Aresta 2010). Moreover, reusing CO_2 not only addresses the balance of CO_2 in the earth's atmosphere but also represents a valuable alternative carbon source to substitute fossil fuels, which are non-sustainable feedstock and will be exhausted in a near future (Aresta 2003; Bhanage and Arai 2014; Centi and Perathoner 2014). Each year about 130 Mt of CO_2 is already used to produce useful chemicals such as urea, salicylic acid, cyclic carbonates and polycarbonates (Alper and Orhan 2017).

One of the most attractive processes of CO_2 fixation is the atom-economical synthesis of cyclic organic carbonates by cycloaddition of CO_2 to epoxides, which has been industrialized for more than 50 years (Cooper and Myri 1956; Peppel 1958; Alves et al. 2017). This reaction represents a greener and safer alternative to the conventional route from diols and highly toxic phosgene (Comerford et al. 2015). Cyclic organic carbonates are of particular interest due to its wide range of applications (North 2013), e. g. as polar aprotic solvents (Schäffner et al. 2010; Alder et al. 2016; Bello Forero et al. 2016), electrolytes in lithium-ion batteries (Zhao et al. 2014), industrial lubricants (Shaikh and Sivaram 1996), monomers for polymer synthesis (Gennen et al. 2017; Gregory et al. 2017; Ruiz et al. 2017) and

as useful intermediates for the preparation of a large variety of organic chemical products (Guo et al. 2018).

During the last two decades, a variety of catalysts have been employed for the synthesis of cyclic carbonates from CO_2 and epoxides, including metal-based catalytic systems such as metal-organic complexes (Meléndez et al. 2007; Decortes et al. 2010; Ema et al. 2014; Maeda et al. 2015; Comerford et al. 2015; Cuesta-Aluja et al. 2016), metal-organic frameworks (Beyzavi et al. 2015; Nguyen et al. 2018), metal oxides (Yamaguchi et al. 1999), metal chlorides (Wilhelm et al. 2014), and organocatalysts such as organic salts (Caló et al. 2002; Cokoja et al. 2015; Fiorani et al. 2015; Hua and Roy 2016), ionic liquids (Sun et al. 2005; He et al. 2014; Xu et al. 2015; Chen and Mu 2019) and hydrogen bond donors compounds (HBDs) (Roshan et al. 2014; Sopeña et al. 2015; Martínez-Rodríguez et al. 2016; Arayachukiat et al. 2017; Liu et al. 2018). Recent efforts in this area has been oriented to find catalysts based on natural sustainable products such as amino acids (Tharun et al. 2014; Roshan et al. 2014), chitosan derivatives (Sun et al. 2012; Taheri et al. 2018) or naturally occurring carboxylic acids (Arayachukiat et al. 2017). Among natural products, biopolymers derived from lignocellulosic wastes are attractive materials for its abundance and low cost. The -OH groups present in the main components of the lignocellulosic materials, cellulose (40–60%), hemicellulose (20–40%) and lignin (10–24%) (Fig. 1, Belgacem and Pizzi 2016; Putro et al. 2016), act as HBD to activate the epoxides to react with carbon dioxide.

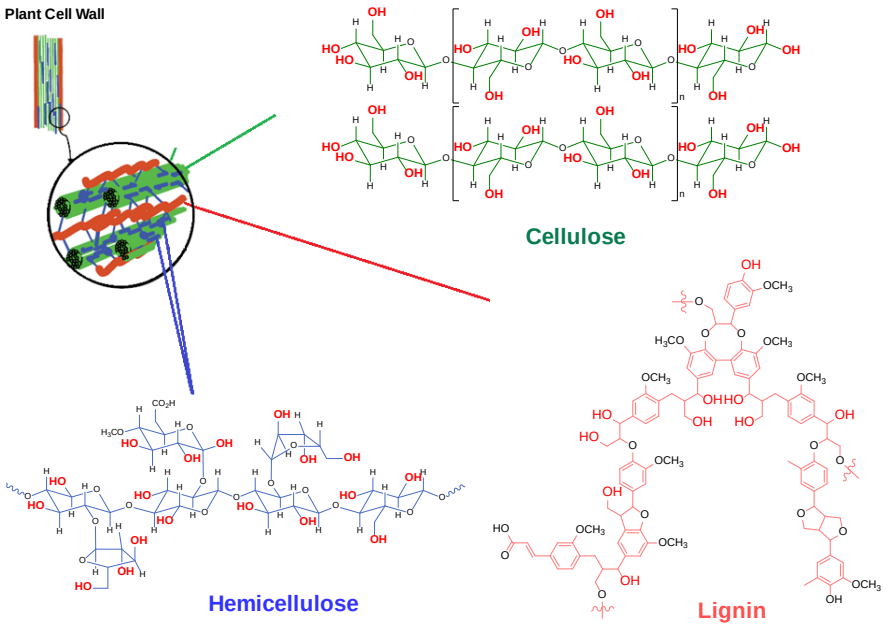

Fig. 1. Lignocellulosic biomass composition

In this context, Wu et al. reported a cooperative green catalyst based on lignin and potassium iodide (KI) in the chemical fixation of CO_2 with epoxides to form cyclic carbonates at 140 ºC and 1.0-4.0 MPa (Wu et al. 2013). For their part, Sun et al. performed the reaction with high activity and selectivity using an environmentally benign catalytic system consisting of 1,8-diazabicyclo[5.4.0]-undec-7-ene (DBU) and cellulose (Sun et al. 2014). Chen et al. opened a new way for a simple and highly efficient utilization of lignocellulosic biomass as a potential alternative in green organic synthesis and catalysis (Chen et al. 2015). They reported on a green and an efficient catalytic system consisting of sugarcane bagasse and KI for cycloaddition of carbon dioxide to epoxides and aziridines at 120 ºC and 2 MPa of pressure. Recently, we used also sugarcane bagasse in combination with tetrabutylammonium bromide (TBAB) as a catalyst for the synthesis of methyl 2,3-carbonyldioxynonanoate by cycloaddition of carbon dioxide to 2,3-epoxynonanoic methyl ester (Ruiz et al. 2017). This catalytic system has provided similar or even better results than metal-based catalytic systems such as Ytterbium trifluoromethanesulfonate ($Yb(OTf)_3$), 2-bis(aminopyridinium) tetrachlorozincate ($[pyNH_2]_2[ZnCl_4]$) and [N,N'-bis(3,5-di-tert-butylsalicylene)-2-aminobenzyl-amino]chloridoaluminium ([Al(salabza)Cl]) in combination with TBAB. In addition, it could be recycled several times without significant loss of activity and selectivity.

Herein we report the performance of various lignocellulosic wastes **1-7** (Scheme 1) in combination with the nucleophiles dimethylaminopyridine (DMAP), 1,8-diazabicyclo[5.4.0]undec-7-ene (DBU), tetrabutylammonium iodide (TBAI), tetrabutylammonium bromide (TBAB) and potassium iodide, as inexpensive, renewable and green catalysts for the synthesis of cyclic carbonates by cycloaddition of CO_2 to epoxides (Scheme 1). The effect of temperature, nucleophile and CO_2 pressure on the catalytic activity was studied, and theoretical calculations based on Density Functional Theory (DFT) have been performed to propose a reaction mechanism.

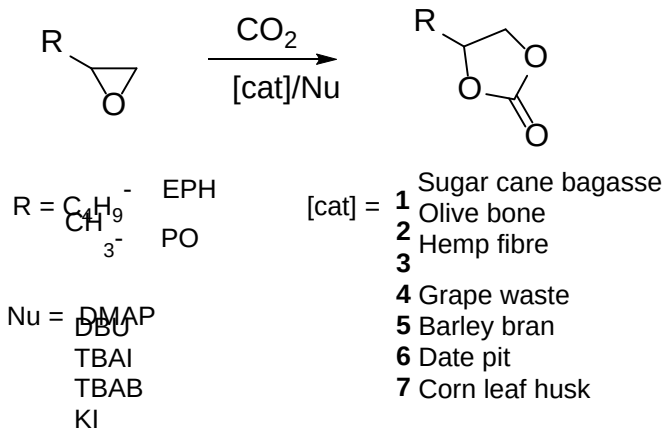

Scheme 1. Synthesis of cyclic carbonates form 1,2-epoxihexane (EPH) and propylene oxide (PO)

Materials and methods

Chemicals and techniques

Chemicals were purchased at Sigma–Aldrich and used as received. Carbon dioxide (SCF Grade, 99.9993%, Abelló Linde) was used introducing an oxygen and moisture trap in the line (Agilent Technologies). NMR spectra were recorded in $CDCl_3$ at 400 MHz Varian spectrophotometer with tetramethylsilane as an external standard. Chemical shifts were expressed in δ (ppm) relative to the resonance. Scanning Electronic Microscopy (SEM) images were performed in an FEI Quanta 600 electronic microscopy coupled with an X-ray detector Oxford Instruments for Energy-dispersive X-ray spectroscopy (EDX) measurement. SEM images were collected at 0.68m Torr, 15 kV high voltage, a working distance of 9.4 mm and magnification of 200x and 3000x. Fourier-transform Infrared spectroscopy (FTIR) spectra were recorded in an FTIR JASCO 6700 equipment in ATR mode 4000-400 cm^{-1}.

Vegetal wastes

Vegetal wastes **1**, **5**-**7** were obtained from small street markets in the province of Tétouan, while samples **2**-**4** were obtained from local suppliers in the Bni Aarouss rural area in the province of Larache (northern Morocco). All vegetal wastes were cleaned manually and dried by exposure to the sun, then chopped to small pieces. Finally, they were milled into powder using a domestic electric grinder. Barley bran

(**5**) was kept as it was. Before using them as catalysts, all vegetal wastes were screened to 14-16 mesh (1,00-1,18 mm), were dewaxed in a Soxhlet extractor with toluene ethanol (2:1 v/v) for 12 h and then dried under vacuum at 60 ºC according to a described procedure (Chen et al. 2015).

Preparation of silica gel-supported TBAB

Silica gel-supported TBAB was prepared according to a reported method (Tundo and Selva 2005). In a typical procedure, 1 g silica-gel (chromatography grade, SDS, Chromagel 60Å CC, 35-70 μm, pore diameter 60 Å, specific surface area 550 m^2 g^{-1}) was added to a solution of TBAB (0.248 g, 0.77 mmol) in MeOH (10 mL) and the resulting suspension was stirred for 15 min. Then, the solvent was evaporated and the solid was heated at 100 ºC in an oven for 15 h.

General procedure for the synthesis of cyclic carbonates

The catalytic tests were carried out in a 100 mL Berghof autoclave with heating through an oil bath. In a typical experiment, the vegetal residue (0.150 g, 6% w/w respect to the substrate 1,2-epoxyhexane), the nucleophile (0.112 mmol, 0.47 mol%) and the substrate (24 mmol) were introduced in the autoclave. The autoclave was closed and vented with 2-3 bar of CO_2. Then, it was pressurized with CO_2 at the desired pressure and introduced in the preheated bath. Reaction temperature indicated in the tables refers to the temperature inside the reactor. After the reaction time, the reactor was cooled down to room temperature with an ice/NaCl bath and slowly depressurized. The conversion (%) was determined by ^{1}H NMR spectroscopy of the crude mixture by the integral ratio between alkene oxide and cyclic carbonate signals. The reaction mixture was filtered to remove the catalyst and washed with ethyl acetate. The product was obtained by evaporation of the solution. The reactions were run in duplicate or until consistent results.

Recycling experiments

After the first catalytic experiment, propylene carbonate was distilled under vacuum. The catalytic mixture was dried off at vacuum and reused for a subsequent cycle.

Chemical analysis of biomass samples

To determine the lignin and holocellulose content the vegetal samples **2-5** were treated as described above. Acid-insoluble lignin content (AIL) analysis of the samples was performed by conventional TAPPI T222 method (Ioelovich 2015). The waste (600 mg) was treated with 72% w/w sulphuric acid (6 mL) at 30 ºC for 1 h; then the concentrated acid was diluted with water to obtain a 3% w/w solution and was refluxed for 1 h. The suspension was cooled down and filtered through glass-filter (n. 3). The sediment of lignin was washed on the filter with water up to pH=7 and then dried at 100 ºC for 4 h. The percentage of AIL in the extracted biomass sample was calculated by the equation: AIL = 100% (P - Pt)/Ps where P is the weight of dry lignin together with glass filter; Pt is the weight of empty glass filter, and Ps is the weight of extracted and dried biomass sample. The filtrate was kept for analysis of the acid-soluble lignin content by UV-absorption at 205 nm. When the absorbance of the direct solution was higher than 1.2 AU the solution was diluted. The content of acid-soluble lignin (ASL) was determined by Beer's law ($A=\varepsilon \cdot c \cdot l$, where ε: absorptivity 110 $L \cdot g^{-1}\, cm^{-1}$, c: concentration $g \cdot L^{-1}$, l: optical path cm) (Hatfield and Fukushima 2005).

The holocellulose content (HC) was determined according to literature data (Sun et al. 2014). The extracted biomass sample (1 g) was placed into a 250 mL round bottom flask with a refrigerant, and then 32 mL distilled water, 0.3 g sodium chlorite ($NaClO_2$) and 3-6 drops of glacial acetic acid were added into the flask. The system was heated at 80 ºC while stirring. After 1 h an additional portion of 0.3 g sodium chlorite and 3-6 drops of glacial acetic acid was added and the treatment was repeated up to 4 additions of sodium chlorite and glacial acetic acid. After cooling at room temperature, the dispersion of holocellulose was filtered through a glass filter (n. 4) and washed with water and acetone. The washed holocellulose was dried at 100 ºC for 1 h to constant weight. The percentage of holocellulose in the extracted biomass sample was calculated by the equation: HC = 100% (P - Pt)/Ps

where P is the weight of dry holocellulose together with glass filter; Pt is the weight of empty glass filter and Ps is the weight of extracted and dried biomass sample.

Computational methods

The geometry optimizations and frequency calculations were performed using the Density Functional Theory (DFT) as implemented in Gaussian 16. The B3LYP functional was chosen to be used due to its good performance in similar systems. The D3 version of Grimme's empirical dispersion was plugged into the method to correct the basis set superposition error (BSSE) among the reaction moieties. The 6-31+G(d,p) basis set was used for main group atoms and LanL2DZ for heavier Br atom. This level of calculation will be represented from now on as *Level-1*. To refine the final energies, single-point energy calculations were performed on the previously optimized geometries using B3LYP-D3BJ (Hong et al. 2018; Li et al. 2019) method with 6-311+G (2df,p) basis set for main group atoms and SDD basis set for Br atom. This more consuming level of calculation will be denoted as *Level-2.*

The Solvation Model Based on Density (SMD) was used to describe the reaction media (Marenich et al. 2009) as a polarizable continuum. In the theoretical study, to decrease computational costs, propylene oxide (PO) was selected as a model epoxide. To reproduce its effect as a solvent, instead, we took 2-butanol from the Gaussian library, given that it has similar properties to PO, with a dielectric constant $\varepsilon = 15.94$ ($\varepsilon = 16$ for PO) and a refractive index, $\eta_D = 1.397$ ($\eta_D = 1.366$ for PO) (Bhanage and Arai 2014; Frisch et al. 2016; Hong et al. 2018).

To afford geometry optimization calculations, the geometries of cellulose and lignin (see models used further down) were frozen except for the hydroxyl groups that could potentially interact with the substrates. The skeleton geometry used was optimized in a calculation where the catalyst was the only species in the system, considering the PO solvent as a polarizable continuous media.

To take into account the entropic effect, the reaction barriers are reported in terms of free energy of activation ($\Delta G^{\ddagger}$) which is the free energy difference between transition states and the previous stable structure along the reaction path (reactants or intermediates). The Gibbs free energy changes ΔG are calculated as

$$\Delta G = \Sigma(\varepsilon_0 + ZPVE + G_{corr})_{product} - \Sigma(\varepsilon_0 + ZPVE + G_{corr})_{reactant}$$

where ε_0 is the total electronic energy (calculated in this case at *Level-2*), ZPVE is the zero-point vibrational energy and G_{corr} is the thermal correction to Gibbs free energy, both calculated at *Level-1*. Final values of ΔG in the profiles also include a correction of 1.89 kcal/mol, for each reactant moiety. This value comes from the term $RT\ ln\ (c_s / c_g)$, that accounts for the change on the Gibbs free energy value due to the change from the standard condition in the gas phase (1 atm) to the standard state in solution (1 mol L^{-1}) (Yu et al. 2017). For this reason, c_s is the standard molar concentration in solution (1 mol L^{-1}) and c_g is the standard molar concentration in the gas phase (0.0446 mol L^{-1}), considering the reaction at 298 K, and being R the gas constant.

The reference energy of the reactants was obtained computing the energy of CO_2 in an independent calculation, considering that this reactant does not interact initially with the species formed by the catalytic system with the PO substrate and the bromide ion. However, all the other intermediates, transition states, and products were studied including all the moieties together.

The intrinsic reaction coordinate (IRC) method was used to confirm that the TS located connect the desired minima. However, in the cases where the IRC calculation did not converge, the appropriateness of the transitions states was checked by the analysis of the reaction coordinated given by the normal mode with imaginary frequency.

All the calculations were performed using computational chemistry package Gaussian 16 (Frisch et al. 2016). The atomic charge distributions were calculated by Mulliken analysis.

Comparison of our results with previously published data for the reaction catalysed by TBAB gave noticeable discrepancies which source was analysed in detail. Test calculations (reported in Supplementary Information) indicated that small numerical differences were due to different versions of the computational program used and to the solvent considered, but the most significant discrepancy came from the solvent model used, PCM (Polarizable Continuum Model) in previous calculations *vs* the more recent SMD one used in this work.

For cellulose/TBAB and lignin/TBAB reactions, TBAB was represented only by the bromide anion, as done in previous works (Hu et al. 2018). Preliminary test calculations performed by our group showed that the presence of the cation in the computational system did not noticeably modify the energy profile. So, to avoid

increasing the computational cost, the cation was not included in these model systems.

Results and discussion

Catalytic studies

The catalytic activity of the vegetal wastes in the fixation of CO_2 into epoxides was first explored in the reaction of CO_2 with 1,2-epoxyhexane as a benchmark substrate at mild conditions (3 % w/w vegetal waste, 0.93 mol% nucleophile, 65 ºC, 20 bar CO_2 and 6 h) using previously reported sugarcane bagasse (**1**) as catalyst (Chen et al. 2015). Initially, different nucleophiles were explored including halide salts (KI), ammines 1,8-diazabicyclo[5.4.0]undec-7-ene (DBU) and dimethylaminopyridine (DMAP), and the quaternary ammonium salts tetrabutylammonium bromide (TBAB) and tetrabutylammonium iodide (TBAI). The results are summarized in Table 1. At these mild conditions, sugarcane bagasse activity depends strongly on the nature of the nucleophile. While no activity was detected with the organic bases DMAP and DBU, a moderate conversion was obtained with ammonium salts. Under these conditions, TBAI and TBAB provided the best conversion in the cycloaddition product (15 and 17 % respectively, entries 1 and 2, Table 1), which in all cases, was the only product detected (>99 % according to ^{1}H NMR). When the reaction was carried out using TBAB alone, the conversion was only 11% (entry 3, Table 1), indicating a synergetic effect between **1** and TBAB when both were combined (entry 2, Table 1). Under these mild conditions, the previously reported system **1**/KI (Chen et al. 2015) was not active what evidenced the importance of the right combination of catalyst and nucleophile. The tetrabutylammonium salts are probably more soluble in the epoxide at these conditions and, therefore, are more active.

The effect of temperature and reaction time using TBAB as co-catalyst in the cycloaddition of CO_2 to 1,2-epoxyhexane was then studied. The results are listed in Table 1 (entries 4-7). Increasing the temperature from 65ºC to 75ºC, the conversion reached 33 % after 16 h (entry 7, Table 1). Under the same conditions, the conversion obtained with ground olive bones (**2**) was higher (38% in entry 5, Table 1) and reached a 67 % conversion when the temperature was increased up to 95 ºC (entry 6, Table 1). A conversion of 82 % at >99% selectivity in the cyclic carbonate

was obtained increasing the amount of catalyst (up to 6% w/w) and nucleophile (up to 1.87 mol%) as shown in entry 7 (Table 1).

Table 1. Cycloaddition of CO_2 to 1,2-epoxyhexane using catalysts **1**-**2**/nucleophile (Nu).[a]

Entry	Cat	Nu	T (ºC)[b]	t (h)	Conv (%)[c]
1	**1**	TBAI	65	6	15
2	**1**	TBAB	65	6	17
3	-	TBAB	65	6	11
4	**1**	TBAB	75	6 (16)	20 (33)
5	**2**	TBAB	75	16	38
6	**2**	TBAB	95	16	67
7[d]	**2**	TBAB	95	16	82

[a] Reaction conditions: substrate: 4.8 g (0.048 mol), catalyst: 150 mg (3 % w/w respect to the substrate), Nu: nucleophile: 0.45 mmol (0.94 mol % respect to the substrate), 3h, 20 bar CO_2.

[b] internal temperature

[c] Conversion determined by NMR

[d] catalyst: 6 % w/w respect to the substrate, TBAB: 1.87 mol% respect to the substrate

Subsequently, we investigated the effect of the reaction pressure in the cycloaddition of CO_2 to 1,2-epoxyhexane with catalytic system **2**/TBAB under the conditions of 6 % catalyst and 1.87 mol % TBAB at 95 ºC (Fig. 2). The effect of the CO_2 pressure in the conversion in the range of 10-30 bar is low. At lower pressure (1 bar) the conversion dropped although the system was still active and produced 68 % conversion in the cycloaddition product after 48 h. Therefore, a pressure of 10 bar was used for the following experiments.

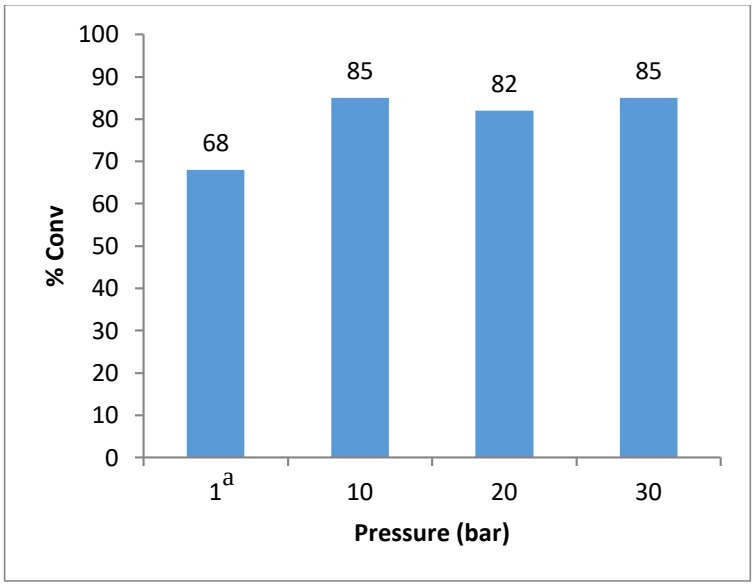

Fig. 2. Effect of P(CO_2) on % conversion. Reaction conditions: epoxyhexane (0.024 mol), catalyst **2**: 150 mg (6 % w/w respect the substrate), TBAB: 0.45 mmol (1.87 mol% respect to the substrate), T= 95 °C, t= 16 h. Conversion determined by ^{1}H NMR. Yield isolated. [a] t= 48 h

Next, the amount of TBAB was optimized using a catalyst **2** loading of 6% (Fig. 3). It was found that the conversion was still high (76%) at a very low concentration of TBAB (0.47 mol% respect to the substrate, Fig. 3). At 0.47 mol% of TBAB, the blank experiments using **2** or TBAB alone confirmed the cooperative effect of the two components in the catalytic reaction. Such catalytic activity of tetraalkylammonium salts bearing halides as counterions has been reported earlier (Caló et al. 2002). The combination of lignocellulosic waste **2** and TBAB resulted in a considerable increase in the conversion (up to 76%) that is probably due to a synergetic effect. Activation of the epoxide by hydrogen bond formation with the abundant hydroxyl groups of lignocellulosic waste **2** may facilitate the nucleophilic attack of the bromide anion of TBAB, by which the ring of epoxide is opened easily and therefore the reaction with CO_2 is accelerated (Shaikh et al. 2018) (Fig. 4) as it will be discussed below. Nevertheless, when higher loading of TBAB was used (1.87 mol %) the vegetal catalyst did not affect the conversion. Then, with the right combination of catalyst and nucleophile, the amount of TBAB can be reduced to less than 0.5 mol% by using instead cheap, disposable and harmless materials.

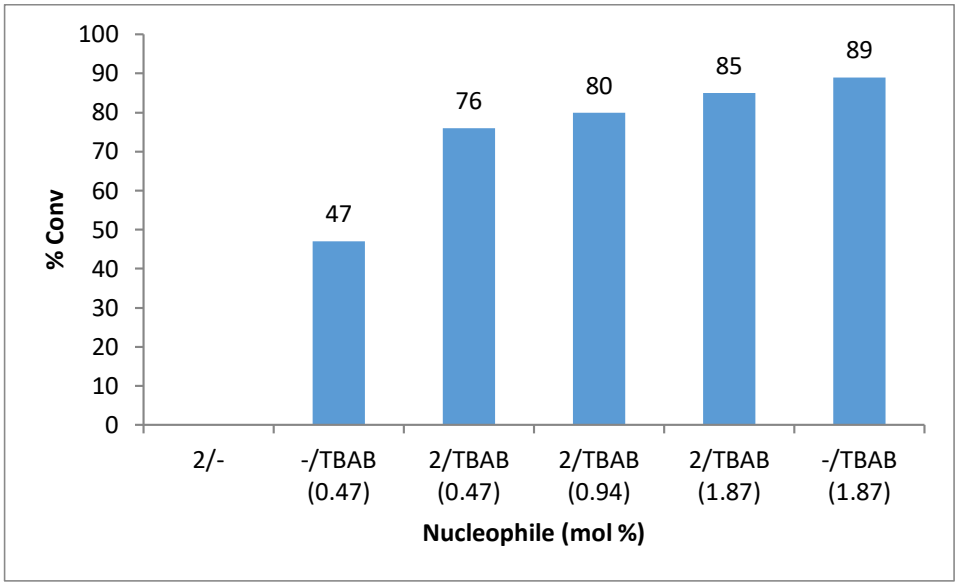

Fig. 3. Effect of molar ratio of TBAB. Reaction conditions: 1,2-epoxyhexane (0.024 mol), catalyst **2**: 150 mg (6% w/w respect the substrate), T= 95 °C, P(CO_2)= 10 bar, t= 16 h. Conversion determined by ^{1}H NMR.

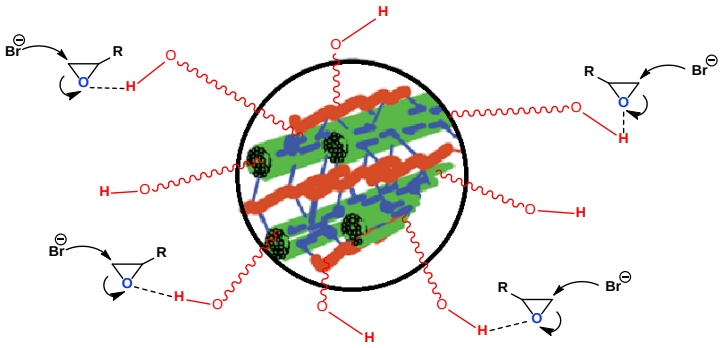

Fig. 4. Proposal for the activation of the epoxide by hydrogen bond formation.

These preliminary experiments allowed to set the reaction conditions at 6 % w/w catalyst, 0.47 mol% TBAB, 95 ºC, 10 bar and 16 h. Under these conditions, the catalytic activity of a series of lignin-containing wastes **3**-**7**, largely produced from processed vegetal industries, was studied using TBAB as a nucleophile (Fig. 5). Corn leaves (**7**), olive bones (**2**), date pit (**6**) and grape waste (**4**) residues based catalytic systems had high activity and selectivity in the formation of 1,2-hexyl carbonate (>70%) and propylen carbonate (76-84%). The blank experiments using TBAB as catalyst confirmed the synergic effect of the use of this binary catalytic systems increasing the conversion by 40-80%.

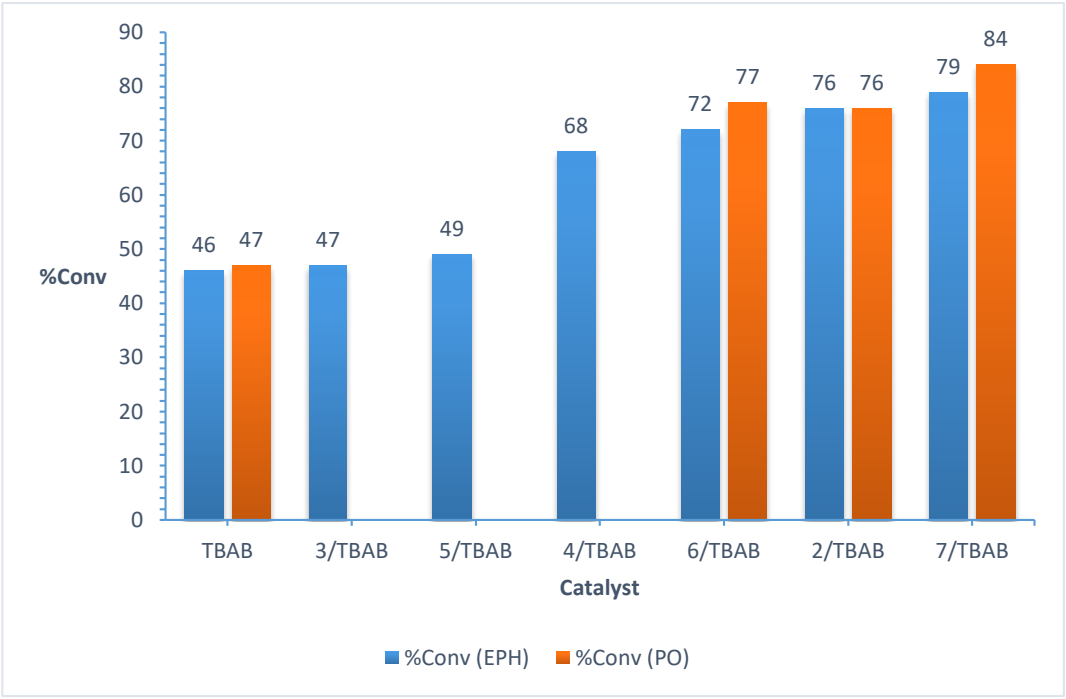

Fig. 5. Substrate conversion by various lignocellulosic residues in addition to TBAB. Reaction conditions: substrate: 0.024 mol (EPH=1,2-epoxyhexane; PO= propylen oxide), cat: 150 mg (6 % w/w), co-cat: 0.112 mmol (0.47 mol%) respect to the substrate. T=95 ºC, t = 16 h, P=10 bar CO_2. Conversion determined by ^{1}H NMR.

Catalyst stability and recycling

The stability of the vegetal residues during the catalytic reaction was analysed by comparative the Scanning Electronic Microscopy (SEM), Energy-dispersive X-ray spectroscopy (EDX) and Fourier-transform Infrared spectroscopy (FTIR) of the fresh vegetal residues and those after the reaction (see Supplementary Information). The fresh materials exhibited characteristic peaks in the FTIR at 3303-3200 cm^{-1} (-OH), 2930-2900 cm^{-1} (C-H), 1640-1600 cm^{-1} (C=C) and 1029-1000 cm^{-1} (C-O) (Caulfield 2005). In the samples of the more active materials **2**, **4**, **6** and **7,** after the catalytic run, a new peak at 1781-1788 cm^{-1} appeared which was attributed to -C=O carboxylic groups formed by carboxylation with CO_2 of the -OH groups (Chen et al. 2015). The interaction of CO_2 with the -OH functionalities to form carboxylic groups may also favour the insertion of CO_2 to the epoxides. The SEM images (see Supplementary Information) showed that the morphology of the surfaces of the bulk materials did not change after catalysis except for the samples of the less active systems, hemp fibre **3**, which increased its fibrous appearance (Fig. S3), and barley bran **5**, which reduced the size of the particles (Fig. S7). The EDX analysis of the samples did not detect nitrogen after the catalytic reaction, suggesting that the ammonium salt, TBAB, was not retained by the vegetal material after the separation of the carbonate. To optimize the retention of the nucleophile on the solid support, TBAB was anchored in silica gel by impregnation of the support with a solution of the ammonium salt in MeOH (TBAB@SiO_2), as reported previously (Tundo and Selva 2005). The recycling experiments using catalyst **2** in combination with supported TBAB (**2**/TBAB@SiO_2) were done for the cycloaddition of CO_2, as limiting reactant, to propylene oxide in excess in a batch reactor (maximum % conversion < 100 %). The propylene carbonate and remaining substrate were separated by distillation after the reaction time and the dried catalyst was reused without further purification and without the addition of fresh TBAB. The conversion was maintained during two runs, indicating that the silica-gel retained the ammonium salt supported. Nevertheless, the conversion dropped in the third run

probably due to some TBAB leaching (Fig. 7). Since the recyclability of TBAB supported on SiO_2 has been previously reported (Tundo and Selva 2005) this system was not further optimised.

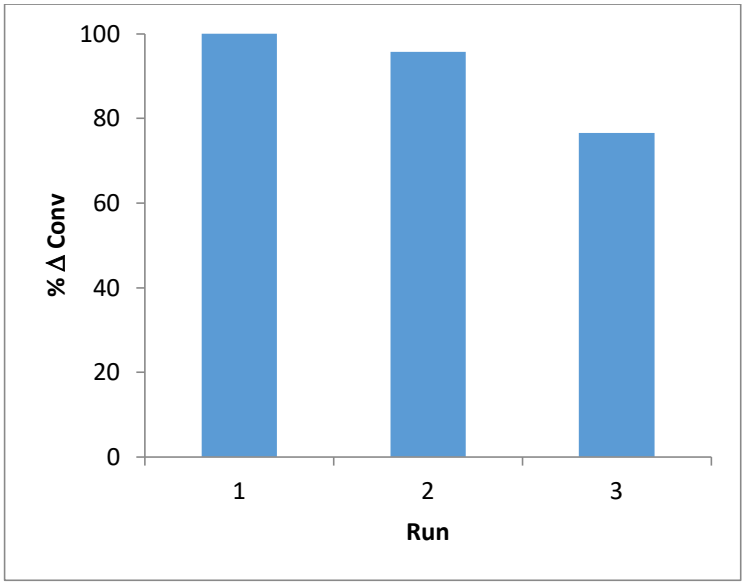

Fig. 6. Recycling of cycloaddition of CO_2 to propylene oxide using catalysts **2**/TBAB@SiO_2. % Δ conversion defined as the relative percentage of conversion respect to the first run. Reaction conditions: substrate: 0.08 mol, **2**: 300 mg, TBAB@SiO_2: 348 mg (0.47 mol %), T=95 ºC, P=10 bar CO_2, 16 h. Conversion determined by ^{1}H NMR.

Mechanistic considerations

Lignin and hollocellulose content of the vegetal residues

To determine the effect on the conversion of the relative content of lignin and cellulose of the vegetal samples, (the main -OH containing components of the lignocellulosic residues) we analysed the total lignin content (TLC) and hollocellulose content (HC) in the vegetal wastes **2**, **3**, **4** and **5** using described methods (Hatfield and Fukushima 2005; Ioelovich 2015). The TLC included the acid-insoluble lignin (AIL) and the acid-soluble lignin content (ASL) obtained by treatment with diluted sulfuric acid. The hollocellulose comprises the cellulose and hemicellulose insoluble content of the samples obtained by treatment with sodium chlorite. The results (Fig. 8) did not show a direct correlation between lignin or holocellulose content and conversion although the samples with higher TLC presented the higher conversion. Thus, catalytic systems **2**/TBAB and **4**/TBAB

with 29 and 51% of TLC respectively provided higher conversion (76 and 68% conversion respectively) than **5**/TBAB and **3**/TBAB with a lignin content 6% and 16% (49 and 47% conversion respectively). When the isolated lignin (AIL) and holocellulose (HC) were checked as catalysts under the same conditions the conversion obtained with lignin/TBAB catalytic system was higher (72%) than the conversion obtained with holocellulose/TBAB and (38%). The Brönsted acidity of the hydroxyl groups (expressed as pK_a) of hydrogen bond donor catalysts has been related to the catalytic activity in the cycloaddition of CO_2 to epoxides (Yingcharoen et al. 2019). Thus, an ideal range of 9 <pKa<11 has been identified in which fall phenolic derivatives, such as the ones contained in lignin structure. Nevertheless, there can be other factors, suggested by the computational results (see discussion further down), that could also increment the catalytic activity of lignin relative to holocellulose.

Moreover, high or low holocellulose content does not seem to be related with high conversion since **2**/TBAB with 71% of holocellulose gives a 76% conversion while the conversion obtained using **3**/TBAB with 79% holocellulose was 47%. Then, it may be the combination of both components with the nucleophile TBAB what determines the catalytic activity.

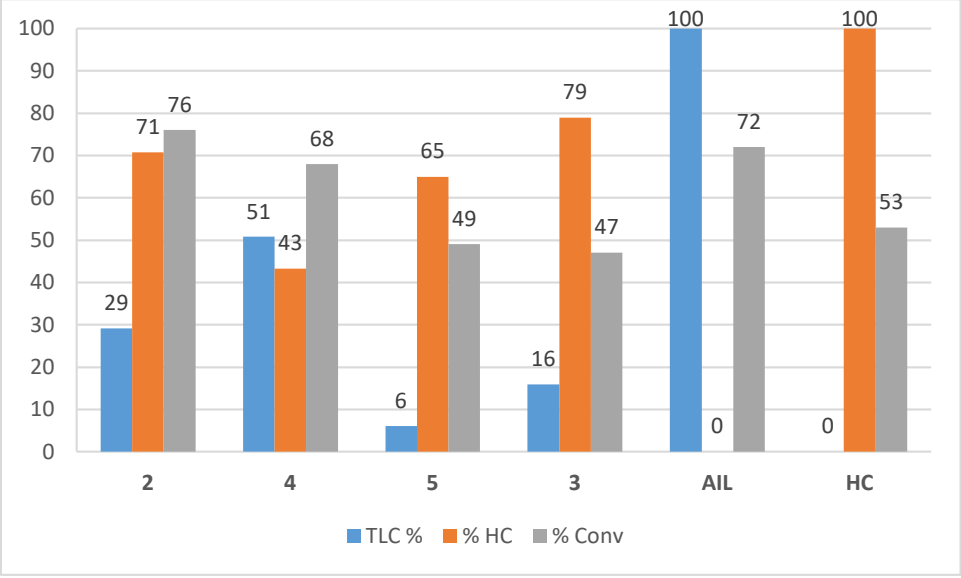

Fig. 7. Total lignin content (TLC) (%) and holocellulose content (HC) (%) of the residues **2**,**3**, **4** and **5** and conversion (%) obtained in the cycloaddition of CO_2 to 1,2-epoxyhexane. Reaction conditions: substrate: 1,2-epoxyhexane 2.4 g (0.02 mol), cat: 150 mg (6% w/w), co-cat: 0.112 mmol (0.47 mol%) respect to the substrate. T = 95 ºC, t = 16 h, P = 10 bar CO_2. Conversion determined by ^{1}H NMR.

DFT calculations

To get more information about how the two components of lignocellulose, namely cellulose and lignin, may act as catalysts for this reaction, the mechanism of the reaction was studied with DFT model calculations, by exploring the potential energy surface (PES) of the ground states of these systems along the most plausible paths. Cellutriose (CtS) consisting of three β-D-glucose units connected through β-1,4-glycosidic linkages (Fig. 9a), was chosen as the model of cellulose in the basis of previous studies (Watts et al. 2014). The lignin of the lignocellulosic residues was modelized by four monomeric coniferyl alcohol motifs linked via β-O-4 ether bonds (LiG, Fig. 9b), also in the basis of previous studies (Yang et al. 2019). The profiles of the reactions of PO and CO_2 with a) CtS + bromide and b) LiG + bromide were obtained. We also modelled the reaction only with TBAB as a catalyst to compare with previous studies (Hu et al. 2018; Li et al. 2019; Yang et al. 2019) (see details in Supplementary Information). Test calculations showed no interaction between TBA^+ and PO. Since the cation TBA^+ does not play any role, only the Br^- anion was included in the computed system (see Supplementary Information).

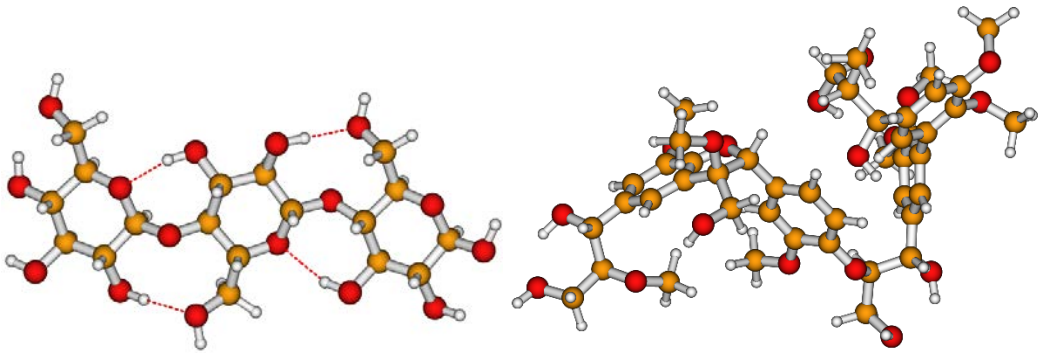

(a) (b)

Fig. 8. Models for a) cellulose (cellutriose, CtS) and b) lignin (coniferyl alcohol derivative, LiG)

Based on reported studies (Li et al. 2019), the assumed reaction pathway using TBAB as catalyst includes the following steps: PO ring-opening by the nucleophile Br^-, CO_2 insertion and the ring closure to form the cyclic carbonate. In substituted epoxides ring-opening may take place at C_α, the more substituted, or C_β, being the nucleophile attack to the less hindered non-substituted carbon C_β the favoured in this case (Foltran et al. 2014; Hu et al. 2018). The rate-determining step for TBAB

catalyst is the initial ring-opening of the epoxide by the nucleophilic attack of Br^- with an activation energy $\Delta G^{\#}$= 16.09 kcal mol^{-1} (see Supplementary Information). We then studied the CtS/TBAB and LiG/TBAB catalysed reactions. The models were selected considering the presence of -OH groups in close proximity (Wang 2015; Liu et al. 2019). To analyse the interaction between the catalyst (CtS or LiG) and the substrate (PO), the last one was located in different positions around the biopolymer, always close to the -OH groups. In this way, we identified the active sites that showed the strongest interaction with the substrate to select the most appropriate reaction path to follow. Both catalysts differ in that CtS is a 1,2-diol (with two vicinal –OH groups) whereas the active sites of LiG contain two –OH groups in a 1,3– relative positions. Figures 10 and 11 show the reaction profiles found for reactions with CtS and LiG respectively, together with schematic representations of the geometries of the critical points located. More detailed geometries can be found in Figures S2 and S3 of the Supplementary Information.

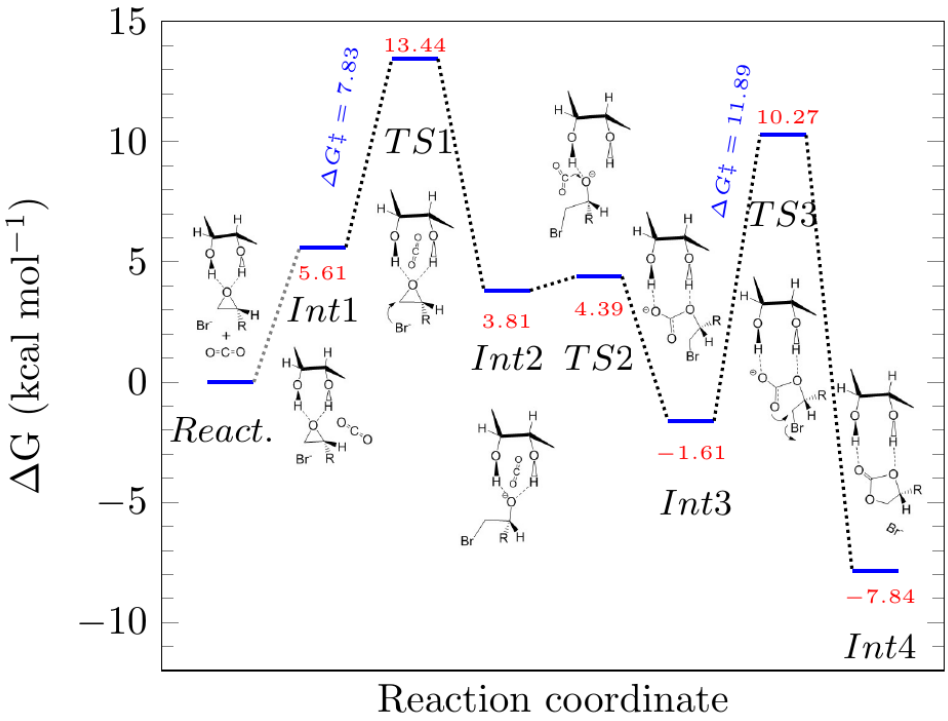

Fig. 10. Gibbs free energy profile in the CtS/TBAB-catalyzed CO_2 cycloaddition to PO. Only the active site of the biopolymer (CtS) is represented in the models for clarity.

Given that in the experimental setup the epoxide is the solvent, the interaction between the vegetal material and the epoxide is considered to exist before the actual reaction begins, so the reactants are modelled with a biopolymer-PO adduct plus

Br^- and CO_2. In both CtS and LiG cases, the catalytic cycle initiates with the interaction of the epoxide with two consecutive hydroxyl groups of the vegetal material through two H-bond (Int1, Fig 10 and 11). This activates the epoxide and decreases the ring-opening energy barrier to 7.83 and 9.94 kcal/mol for CtS/TBAB and LiG/TBAB respectively, in comparison to that of the reaction catalysed by TBAB (16.09 kcal mol^{-1}). The intermediate Int1 formed with LIG is more stable than the one formed with CtS by 1.24 kcal/mol which suggests a slightly more efficient interaction of the epoxide with the LiG.

Next step, the insertion of CO_2 to Int2 to form Int3, (Figure 10 and 11) takes place with a very low barrier (0.58 and 2.57 kcal/mol for CtS/TBAB and LiG/TBAB respectively). The insertion occurs through a CO_2-adduct with the electron-rich alkoxide species (TS2, Figures 10 and 11) that breaks the linearity of CO_2, given the gradual change of the C atom hybridization from sp to sp^2. The O-C-O angle, ~161º at TS2, changes to ~129º at Int3 for both models and it makes CO_2 a C-electrophile leading to cyclic carbonate (Aresta et al. 2016). Bromide leaving and ring-closing of the carbonate is the highest energy barrier for the CtS/TBAB catalytic system ($\Delta G^{\#}$= 11.89 kcal/mol). Despite TS2 being more energetic than TS3, the height of the latter barrier is larger due to the stability of the precedent intermediate, Int3, relative to that on Int2. On the other hand, for the LiG/TBAB system the last barrier of the mechanism is comparable ($\Delta G^{\#}$= 9.20 kcal/mol) with the barrier of the ring-opening step. In both cases, the intermediate reached (Int4), is the most stable species of the profile (-7.84 and -12.82 kcal mol^{-1} for CtS/TBAB and LiG/TBAB respectively).

To close the catalytic cycle, the product must be released, replaced by a new substrate molecule (PO) at the active site. To model this step, another PO and CO_2 molecules should be included in the model, which makes the simulation unpractical. The global comparison of the profiles obtained for the cellulose and lignin models catalysed reaction shows that the initial part of the reaction is very similar in both systems (from reactants to Int2), from the energetic (Figures 10 and 11) as well as from the geometrical point of view (Figures S2 and S3). The average energy difference in this part of the reaction costs less than 1 kcal mol^{-1}, and the main distances of the reactive species differ less than 0.05Å between systems. On the other hand, larger differences are found between the energies and geometries involved in the last steps of the reaction. The averaged energy difference between

the barriers at this step (TS3) is almost 4 kcal mol^{-1}. Regarding geometries, Int3 shows a non-negligible difference between systems: the $O_{CO2}\cdots C_{PO}$ distance is 0.4 Å larger in the cellulose system than in the lignin one.

This variation can be due to the nature of the H-bond interactions of the catalyst and substrate in the different parts of the reaction. In the initial species (from reactants to Int2), the two hydrogen bonds generated between the catalyst and the substrate are formed with only one oxygen atom, that of the epoxide. On the other hand, from Int3 to products, the two hydrogen bonds are established with two different oxygen atoms, making a more stable species when the lignin is the catalyst. It seems to indicate that the 1,3-relative position of the hydroxyl groups in lignin is more adequate than the 1,2-relative position of these groups in cellulose to facilitate the ring closure of the cyclic carbonate.

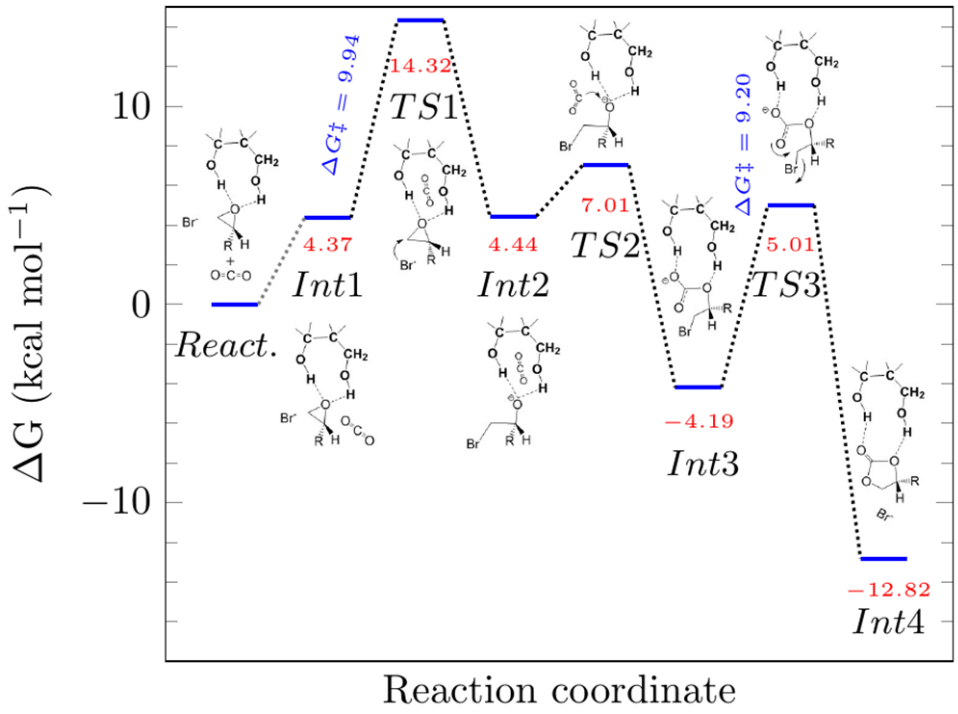

Fig. 11. Gibbs free energy profile for LiG/TBAB-catalyzed CO_2 cycloaddition to PO. Only the active site of the biopolymer (LiG) is represented in the models for clarity.

This hypothesis is supported by the comparison of the energy barrier and catalytic activities of the reactions studied, as is shown in Table 2. Thus, the relative order of activation energies for the model catalytic systems TBAB > CtS/TBAB > LiG/TBAB agrees with the relative order of activity observed experimentally (Table 2). Nevertheless, the conversion obtained with the crude resides **1**-**7**/TBAB are in the range of 47-79%. These values indicate that not only both elements,

cellulosic and lignin fragments, contribute to the activity of the whole material, but also that there can be a synergic catalytic effect due to the interaction between both biopolymers.

Table 2. Conversion to PC and energy barriers calculated by DFT using different catalytic systems.

Catalytic system	Energy barrier (kcal/mol) Ring-opening	Ring-closing	% Conv[a]
TBAB	**16.1**	10.9	47
CtS/TBAB	7.8	**11.9**	53
LIG/TBAB	**9.9**	9.2	72

[a] Reaction conditions: substrate: 1,2-epoxyhexane 2.4 g (0.02 mol), cat **2**: 150 mg (6% w/w), TBAB: 0.112 mmol (0.47 mol%) respect to the substrate. T = 95 ºC, t = 16 h, P = 10 bar CO_2. Conversion determined by ^{1}H NMR.

To sum up, the DFT study shows that the interaction of the –OH groups of the lignocellulosic materials with the reactant system is crucial for the activity of these catalysts. This interaction decreases the energy barrier for the ring-opening of the epoxide by the Br^- and explain why the combination of the lignocellulosic wastes with TBAB is a more active catalyst than TBAB in most of the cases. The interaction of CO_2 with the activated epoxide is the key point for the second step of the reaction. Like in the case of the H-bonds, this is a noncovalent interaction that could be described as a tretel bond, established between the C atom of CO_2, a region of positive electrostatic potential (σ-hole), and the negatively charged oxygen of the epoxide. This is another example of the crucial role that noncovalent interactions have in the mechanisms of catalysed reactions, as pointed out lately by several authors (Mahmudov et al. 2019). Regarding the question about which component contributes more to the total activity, although the lignin model in combination with TBAB has the lowest energy barrier and lignin/TBAB is a more active catalyst, other factors such as the diffusivity of the reactants in the solid materials or the interconnection of the lignocellulosic biopolymers in the specific waste may account for the final activity observed.

Conclusion

Cheap and accessible lignocellulosic vegetal wastes in combination with a nucleophile form active catalysts for the cycloaddition of CO_2 to epoxides without the use of added solvents. The adequate combination of the vegetal residue and the nucleophile allowed the use very low nucleophile loading (<0.5 mol%) to obtain alkyl acyclic carbonates such as propylene carbonate and 4-butyl-1,3-dioxolan-2-one selectively. Although the conversions are in general lower than the ones obtained with metal-based catalysts, it has the advantages of very low cost, sustainability (Shaikh et al. 2018) and very simple treatment of the materials. Even more, the vegetal residues were stable under reaction conditions and could be recycled after adequate support of the nucleophile. The mechanistic DFT studies together with the analysis of the lignin and hollocellulose content of the materials let to the conclusion that the 1,2- and 1,3- diol of the cellulose and lignin fragments activate the epoxide by H-bond. The -OH groups present in the hollocellulose and lignin contribute to their activity as catalysts although other factors such as the diffusivity of reactants or the interconnection of the lignocellulosic biopolymers may also contribute.

Acknowledgements

The authors are thankful to *Ministerio de Economia y Competitividad* and AEI/FEDER UE (CTQ2016-75016-R and CTQ2017-83566-P), *Departament d'Economia i Coneixement* (2017 SGR 1472 and 2017 SGR 629) and *Xarxa d'R+D+I en Química Computacional* (XRQTC).

Appendix A. Supplementary data

The xyz coordinates of the DFT calculations of this article can be found in a figshare data repository (See at doi: https://figshare.com/s/84bc57f3018e66bf3618).

References

Alder CM, Hayler JD, Henderson RK, et al (2016) Updating and further expanding GSK's solvent sustainability guide. Green Chem 18:3879–3890. https://doi.org/10.1039/c6gc00611f

Alper E, Orhan OY (2017) CO2 utilization: Developments in conversion processes. Petroleum 3:109–126. https://doi.org/10.1016/j.petlm.2016.11.003

Alves M, Grignard B, Mereau R, et al (2017) Organocatalyzed coupling of carbon dioxide with epoxides for the synthesis of cyclic carbonates: catalyst design and mechanistic studies. Catal Sci Technol 7:2651–2684. https://doi.org/10.1039/C7CY00438A

Arayachukiat S, Kongtes C, Barthel A, et al (2017) Ascorbic Acid as a Bifunctional Hydrogen Bond Donor for the Synthesis of Cyclic Carbonates from CO2 under Ambient Conditions. ACS Sustain Chem Eng 5:6392–6397. https://doi.org/10.1021/acssuschemeng.7b01650

Aresta M (2003) Carbon Dioxide Recovery and Utilization. Springer, Dordrecht

Aresta M (2010) Carbon Dioxide: Utilization Options to Reduce its Accumulation in the Atmosphere. Carbon Dioxide as Chem Feed 1–13. https://doi.org/10.1002/9783527629916.ch1

Aresta M, Dibenedetto A, Quaranta E (2016) The Carbon Dioxide Molecule. In: Reaction Mechanisms in Carbon Dioxide Conversion. Springer Berlin Heidelberg, pp 1–34

Belgacem MN, Pizzi A (2016) Lignocellulosic Fibers and Wood Handbook. Wiley-Scrivener

Bello Forero JS, Hernández Muñoz JA, Jones Junior J, da Silva FM (2016) Propylene Carbonate in Organic Synthesis: Exploring its Potential as a Green Solvent. Curr Org Synth 13:834–846. https://doi.org/10.2174/1570179413999160211094705

Beyzavi MH, Stephenson CJ, Liu Y, et al (2015) Metalâ€“Organic Framework-Based Catalysts: Chemical Fixation of CO2 with Epoxides Leading to Cyclic Organic Carbonates. Front Energy Res 2:1–10. https://doi.org/10.3389/fenrg.2014.00063

Bhanage BM, Arai M (2014) Transformation and Utilization of Carbon Dioxide. Springer-Verlag, Heildelberg

Caló V, Nacci A, Monopoli A, Fanizzi A (2002) Cyclic carbonate formation from

carbon dioxide and oxiranes in tetrabutylammonium halides as solvents and catalysts. Org Lett 4:2561–2563. https://doi.org/10.1021/ol026189w

Caulfield DF (2005) Handbook of Wood Chemistry and Wood Composites. Handb Wood Chem Wood Compos. https://doi.org/10.1201/9780203492437

Centi G, Perathoner S (2014) Green Carbon Dioxide, Advances in CO2 Utilization. Wiley, Hoboken

Chen W, Zhong L, Peng X, et al (2015) Chemical Fixation of Carbon Dioxide Using a Green and Efficient Catalytic System Based on Sugarcane Bagasse - An Agricultural Waste. https://doi.org/10.1021/sc5006445

Chen Y, Mu T (2019) Conversion of CO2 to value-added products mediated by ionic liquids. Green Chem 21:2544–2574. https://doi.org/10.1039/C9GC00827F

Cokoja M, Wilhelm ME, Anthofer MH, et al (2015) Synthesis of Cyclic Carbonates from Epoxides and Carbon Dioxide by Using Organocatalysts. ChemSusChem 8:2436–2454. https://doi.org/10.1002/cssc.201500161

Colmenares JC, Kuna E (2017) Photoactive Hybrid Catalysts Based on Natural and Synthetic Polymers: A Comparative Overview. Molecules 22:790. https://doi.org/10.3390/molecules22050790

Comerford JW, Ingram IDV, North M, Wu X (2015) Sustainable metal-based catalysts for the synthesis of cyclic carbonates containing five-membered rings. Green Chem 17:1966–1987. https://doi.org/10.1039/c4gc01719f

Cooper JF, Myri L (1956) Catalytic process for producing alkylene carbonates. US2773070A

Corma A, Iborra S, Velty A (2007) Chemical Routes for the Transformation of Biomass into Chemicals. Chem Rev 107:2411–2502. https://doi.org/10.1021/cr050989d

Cuesta-Aluja L, Campos-Carrasco A, Castilla J, et al (2016) Highly active and selective Zn(II)-NN′O Schiff base catalysts for the cycloaddition of CO2 to epoxides. J CO2 Util 14:. https://doi.org/10.1016/j.jcou.2016.01.002

Decortes A, Castilla AM, Kleij AW (2010) Salen-complex-mediated formation of cyclic carbonates by cycloaddition of CO2 to epoxides. Angew Chemie - Int Ed 49:9822–9837. https://doi.org/10.1002/anie.201002087

Dong Y, Bi J, Zhu D, et al (2019) Functionalized cellulose with multiple binding sites for a palladium complex catalyst: synthesis and catalyst evaluation in

667 Suzuki–Miyaura reactions. Cellulose 26:7355–7370.
668 https://doi.org/https://doi.org/10.1007/s10570-019-02568-w
669 Ema T, Miyazaki Y, Shimonishi J, et al (2014) Bifunctional Porphyrin Catalysts
670 for the Synthesis of Cyclic Carbonates from Epoxides and CO 2 : Structural
671 Optimization and Mechanistic Study. J Am Chem Soc 136:15270–15279.
672 https://doi.org/10.1021/ja507665a
673 Fiorani G, Guo W, Kleij AW (2015) Sustainable conversion of carbon dioxide:
674 The advent of organocatalysis. Green Chem 17:1375–1389.
675 https://doi.org/10.1039/c4gc01959h
676 Foltran S, Mereau R, Tassaing T (2014) Theoretical study on the chemical
677 fixation of carbon dioxide with propylene oxide catalyzed by ammonium and
678 guanidinium salts. Catal Sci Technol 4:1585–1597.
679 https://doi.org/10.1039/c3cy00955f
680 Frisch MJ, Trucks GW, H.B. Schlegel, et al (2016) Gaussian 16 Rev. B.01
681 Gennen S, Grignard B, Tassaing T, et al (2017) CO 2 -Sourced α-Alkylidene
682 Cyclic Carbonates: A Step Forward in the Quest for Functional Regioregular
683 Poly(urethane)s and Poly(carbonate)s. Angew Chemie - Int Ed 56:10394–
684 10398. https://doi.org/10.1002/anie.201704467
685 Gregory GL, Lopez-Vidal EM, Buchard A (2017) Polymers from sugars: cyclic
686 monomer synthesis, ring-opening polymerisation, material properties and
687 applications. Chem Commun 53:2198–2217.
688 https://doi.org/10.1039/c6cc09578j
689 Guo W, Gómez JE, Cristòfol À, et al (2018) Catalytic Transformations of
690 Functionalized Cyclic Organic Carbonates. Angew Chemie Int Ed 57:13735–
691 13747. https://doi.org/10.1002/anie.201805009
692 Hatfield R, Fukushima RS (2005) Can lignin be accurately measured? Crop Sci
693 45:832–839. https://doi.org/10.2135/cropsci2004.0238
694 He Q, O'Brien JW, Kitselman KA, et al (2014) Synthesis of cyclic carbonates
695 from CO2 and epoxides using ionic liquids and related catalysts including
696 choline chloride-metal halide mixtures. Catal Sci Technol 4:1513–1528.
697 https://doi.org/10.1039/c3cy00998j
698 Hong M, Kim Y, Kim H, et al (2018) Scorpionate Catalysts for Coupling CO 2
699 and Epoxides to Cyclic Carbonates: A Rational Design Approach for
700 Organocatalysts. J Org Chem 83:9370–9380.

https://doi.org/10.1021/acs.joc.8b00722
Hu TD, Sun YW, Ding YH (2018) A quantum-chemical insight on chemical fixation carbon dioxide with epoxides co-catalyzed by MIL-101 and tetrabutylammonium bromide. J CO2 Util 28:200–206. https://doi.org/10.1016/j.jcou.2018.09.027
Hua R, Roy S (2016) Organocatalytic Transformation of Carbon Dioxide. In: Karame I, Srour H (eds) Recent Advances in Organocatalysis. InTech
Ioelovich M (2015) Methods for determination of chemical composition of plant biomass. J SITA 17:208–214
Li X, Cheetham AK, Jiang J (2019) CO2 cycloaddition with propylene oxide to form propylene carbonate on a copper metal-organic framework: A density functional theory study. Mol Catal 463:37–44. https://doi.org/10.1016/j.mcat.2018.11.015
Liu M, Wang X, Jiang Y, et al (2019) Hydrogen bond activation strategy for cyclic carbonates synthesis from epoxides and CO 2 : current state-of-the art of catalyst development and reaction analysis. Catal Rev - Sci Eng 61:214–269. https://doi.org/10.1080/01614940.2018.1550243
Liu N, Xie YF, Wang C, et al (2018) Cooperative Multifunctional Organocatalysts for Ambient Conversion of Carbon Dioxide into Cyclic Carbonates. ACS Catal 8:9945–9957. https://doi.org/10.1021/acscatal.8b01925
Maeda C, Taniguchi T, Ogawa K, Ema T (2015) Bifunctional catalysts based on m-phenylene-bridged porphyrin dimer and trimer platforms: Synthesis of cyclic carbonates from carbon dioxide and epoxides. Angew Chemie - Int Ed 54:134–138. https://doi.org/10.1002/anie.201409729
Mahmudov KT, Gurbanov A V., Guseinov FI, Guedes da Silva MFC (2019) Noncovalent interactions in metal complex catalysis. Coord Chem Rev 387:32–46. https://doi.org/10.1016/j.ccr.2019.02.011
Marenich A V., Cramer CJ, Truhlar DG (2009) Universal solvation model based on solute electron density and on a continuum model of the solvent defined by the bulk dielectric constant and atomic surface tensions. J Phys Chem B 113:6378–6396. https://doi.org/10.1021/jp810292n
Martínez-Rodríguez L, Otalora Garmilla J, Kleij AW (2016) Cavitand-Based Polyphenols as Highly Reactive Organocatalysts for the Coupling of Carbon

735 Dioxide and Oxiranes. ChemSusChem 9:749–755.
736 https://doi.org/10.1002/cssc.201501463
737 Meléndez J, North M, Pasquale R (2007) Synthesis of cyclic carbonates from
738 atmospheric pressure carbon dioxide using exceptionally active
739 aluminium(salen) complexes as catalysts. Eur J Inorg Chem 3323–3326.
740 https://doi.org/10.1002/ejic.200700521
741 Nguyen PTK, Nguyen HTD, Nguyen HN, et al (2018) New Metal-Organic
742 Frameworks for Chemical Fixation of CO 2. ACS Appl Mater Interfaces
743 10:733–744. https://doi.org/10.1021/acsami.7b16163
744 North M (2013) Synthesis of cyclic carbonates from carbon dioxide and epoxides.
745 In: Suib SL (ed) New and Future Developments in Catalysis: Activation of
746 CO2. Elsevier, London, pp 379-413.
747 Peppel WJ (1958) Preparation and Properties of the Alkylene Carbonates. Ind Eng
748 Chem 50:767–770. https://doi.org/10.1021/ie50581a030
749 Putro JN, Soetaredjo FE, Lin SY, et al (2016) Pretreatment and conversion of
750 lignocellulose biomass into valuable chemicals. RSC Adv 6:46834–46852.
751 https://doi.org/10.1039/c6ra09851g
752 Ripple WJ, Wolf C, Newsome TM, et al (2017) World scientists' warning to
753 humanity: A second notice. Bioscience 67:1026–1028.
754 https://doi.org/10.1093/biosci/bix125
755 Roshan KR, Kathalikkattil AC, Tharun J, et al (2014) Amino acid/KI as multi-
756 functional synergistic catalysts for cyclic carbonate synthesis from CO2
757 under mild reaction conditions: A DFT corroborated study. Dalt Trans
758 43:2023–2031. https://doi.org/10.1039/c3dt52830h
759 Ruiz L, Aghmiz A, Masdeu-Bultó AM, et al (2017) Upgrading castor oil: From
760 heptanal to non-isocyanate poly(amide-hydroxyurethane)s. Polym (United
761 Kingdom) 124:. https://doi.org/10.1016/j.polymer.2017.07.070
762 Schäffner B, Schäffner F, Verevkin SP, Börner A (2010) Organic carbonates as
763 solvents in synthesis and catalysis. Chem Rev 110:4554–4581.
764 https://doi.org/10.1021/cr900393d
765 Shaikh A-AG, Sivaram S (1996) Organic carbonates. Chem Rev 96:951–976.
766 https://doi.org/10.1021/cr950067i
767 Shaikh RR, Pornpraprom S, D'Elia V, et al (2018) Catalytic Strategies for the
768 Cycloaddition of Pure, Diluted, and Waste CO2 to Epoxides under Ambient

769 Conditions. ACS Catal 8:419–450. https://doi.org/10.1021/acscatal.7b03580
770 Sopeña S, Fiorani G, Martín C, Kleij AW (2015) Highly Efficient
771 Organocatalyzed Conversion of Oxiranes and CO2 into Organic Carbonates.
772 ChemSusChem 8:3179. https://doi.org/10.1002/cssc.201501195
773 Sun J, Cheng W, Yang Z, et al (2014) Superbase/cellulose: an environmentally
774 benign catalyst for chemical fixation of carbon dioxide into cyclic
775 carbonates. Green Chem 16:3071–3078. https://doi.org/10.1039/c3gc41850b
776 Sun J, Fujita S, Arai M (2005) Development in the green synthesis of cyclic
777 carbonate from carbon dioxide using ionic liquids. J Organomet Chem
778 690:3490–3497. https://doi.org/10.1016/j.jorganchem.2005.02.011
779 Sun J, Wang J, Cheng W, et al (2012) Chitosan functionalized ionic liquid as a
780 recyclable biopolymer-supported catalyst for cycloaddition of CO 2. Green
781 Chem 14:654–660. https://doi.org/10.1039/c2gc16335g
782 Taheri M, Ghiaci M, Shchukarev A (2018) Cross-linked chitosan with a dicationic
783 ionic liquid as a recyclable biopolymer-supported catalyst for cycloaddition
784 of carbon dioxide with epoxides into cyclic carbonates. New J Chem 42:587–
785 597. https://doi.org/10.1039/c7nj03665e
786 Tharun J, Roshan KR, Kathalikkattil AC, et al (2014) Natural amino acids/H2O as
787 a metal- and halide-free catalyst system for the synthesis of propylene
788 carbonate from propylene oxide and CO2under moderate conditions. RSC
789 Adv 40:41266–41270. https://doi.org/10.1039/c4ra06964a
790 Thomas B, Raj MC, B AK, et al (2018) Nanocellulose, a Versatile Green
791 Platform: From Biosources to Materials and Their Applications. Chem Rev
792 118:11575–11625. https://doi.org/10.1021/acs.chemrev.7b00627
793 Tundo P, Selva M (2005) Continuous-flow, gas phase synthesis of 1-chlorobutane
794 (1-bromobutane) from 1-butanol and aqueous HCl (HBr) over silica-
795 supported quaternary phosphonium salt. Green Chem 7:464–467.
796 https://doi.org/10.1039/b418941h
797 Wang J (2015) Hydrogen Bond Donor-promoted Fixation of CO2 with Epoxides
798 into Cyclic Carbonates: Moving Forward. Curr Green Chem 2:3–13.
799 https://doi.org/10.2174/2213346101666140630164855
800 Watts HD, Mohamed MNA, Kubicki JD (2014) A DFT study of vibrational
801 frequencies and 13C NMR chemical shifts of model cellulosic fragments as a
802 function of size. Cellulose 21:53–70. https://doi.org/10.1007/s10570-013-

0128-8

Wilhelm ME, Anthofer MH, Reich RM, et al (2014) Niobium(v) chloride and imidazolium bromides as efficient dual catalyst systems for the cycloaddition of carbon dioxide and propylene oxide. Catal Sci Technol 4:1638–1643. https://doi.org/10.1039/c3cy01057k

Wu Z, Xie H, Yu X, Liu E (2013) Lignin-Based Green Catalyst for the Chemical Fixation of Carbon Dioxide with Epoxides To Form Cyclic Carbonates under Solvent-Free Conditions. ChemCatChem 5:1328–1333. https://doi.org/10.1002/cctc.201200894

Xu B-H, Wang J-Q, Sun J, et al (2015) Fixation of CO 2 into cyclic carbonates catalyzed by ionic liquids: a multi-scale approach. Green Chem 17:108–122. https://doi.org/10.1039/C4GC01754D

Yamaguchi K, Ebitani K, Yoshida T, et al (1999) Mg-Al mixed oxides as highly active acid-base catalysts for cycloaddition of carbon dioxide to epoxides. J Am Chem Soc 121:4526–4527. https://doi.org/10.1021/ja9902165

Yang H, Watts HD, Gibilterra V, et al (2019) Quantum Calculations on Plant Cell Wall Component Interactions. Interdiscip Sci Comput Life Sci 11:485–495. https://doi.org/10.1007/s12539-018-0293-4

Yingcharoen P, Kongtes C, Arayachukiat S, et al (2019) Assessing the pK_a -Dependent Activity of Hydroxyl Hydrogen Bond Donors in the Organocatalyzed Cycloaddition of Carbon Dioxide to Epoxides: Experimental and Theoretical Study. Adv Synth Catal 361:366–373. https://doi.org/10.1002/adsc.201801093

Yu JL, Zhang SQ, Hong X (2017) Mechanisms and Origins of Chemo- and Regioselectivities of Ru(II)-Catalyzed Decarboxylative C-H Alkenylation of Aryl Carboxylic Acids with Alkynes: A Computational Study. J Am Chem Soc 139:7224–7243. https://doi.org/10.1021/jacs.7b00714

Zhao H, Park SJ, Shi F, et al (2014) Propylene carbonate (PC)-based electrolytes with high coulombic efficiency for lithium-ion batteries. J Electrochem Soc 161:194–200. https://doi.org/10.1149/2.095401jes